Neutron beam characterization and neutron yield for $^{9}Be(p, n)^{9}B$ of accelerator-based boron neutron capture therapy using MCNP6, PHITS, and Geant4

Sangmin Lee [a], Hyegang Chang [a], Sung-Joon Ye [a*]
[a]*Program in Biomedical Radiation Sciences, Department of Transdisciplinary Studies, Graduate School of Convergence Science and Technology, Seoul National University, Seoul, Korea*
[*]*Corresponding author: sye@snu.ac.kr*

Abstract: In Korea, an accelerator-based BNCT facility is under construction. This facility is designed to make epithermal neutron beam at the irradiation port by using $^{9}Be(p, n)^{9}B$ nuclear reactions with 10 MeV incident proton beam in beam shaping assembly. In this study, neutron beam characteristics and neutron yield through the beam shaping assembly were characterized by using MCNP6, PHITS, and Geant4. The neutron yield from a simple 2-cm thick beryllium target calculated by MCNP was 7 times higher than other two codes and it was also close to the analytical and experimental value. The epithermal neutron flux calculated by MCNP from the current beam shaping assembly design was 2×10^{9} neutrons/sec/cm^2 and it meets the IAEA guideline ($> 1 \times 10^{9}$ neutrons/sec/cm^2).

1. Introduction

The Boron Neutron Capture Therapy (BNCT) is binary radiation treatment modality. It delivers radiation damage to the tumor cell selectively using ^{10}B compound and neutron beam. The ^{10}B nuclei which have high thermal neutron capture cross-section, release α particle and ^{7}Li ion in $^{10}B(n, \alpha)^{7}Li$ reaction. These products have high linear energy transfer characteristics and their ranges are around single cell diameter (~10 μm) in the tissue. Therefore, BNCT can selectively treat the tumor cell with the targeted boron drug delivery [1]. In the South Korea, accelerator-based BNCT (A-BNCT) facility is under construction aiming to make epithermal neutron source. A-BNCT has advantages over reactor based BNCT, i.e. comfortable accessibility, cheap maintenance costs, simple operation and neutron beam characteristics using $^{9}Be(p, n)^{9}B$ nuclear reaction [2]. Before the accelerator optimization to desired level of proton beam energy and intensity, beam characteristics at the end of the Beam Shaping Assembly (BSA) should satisfy some requirements like beam current ratio from the IAEA report [3], radiation safety & protection and therapeutic effect to the patient. Therefore, we used three different Monte Carlo (MC) codes (MCNP, PHITS and Geant4), which are commonly used to transport radiation [4-6] and characterize the beam property.

The primary object of this study is to transport proton beam through BSA design, characterize the neutron beam property at the irradiation port and compare the neutron yield among the widely used MC simulation codes. The results were also compared with analytic calculation and experimental data.

2. Methods and Results

2.1 BSA design

The BSA (Figure 1) was fully designed and revised by Pohang Accelerator Laboratory (PAL). The 10 MeV proton beam (maximally 8 mA), which have 12×12 cm^2 size of the field will hit and stop in the $19 \times 19 \times 2$ cm^3 beryllium target. The surrounding copper and water pipe removes heat from the target continuously. The other various materials such as lead, iron, aluminum fluoride, lithium fluoride, aluminum, borated polyethylene and tungsten were used as moderator, beam shaper, collimator and shield. The entire dimension of BSA is around $150 \times 240 \times 200$ cm^3 and the beam exit is 12 cm in diameter.

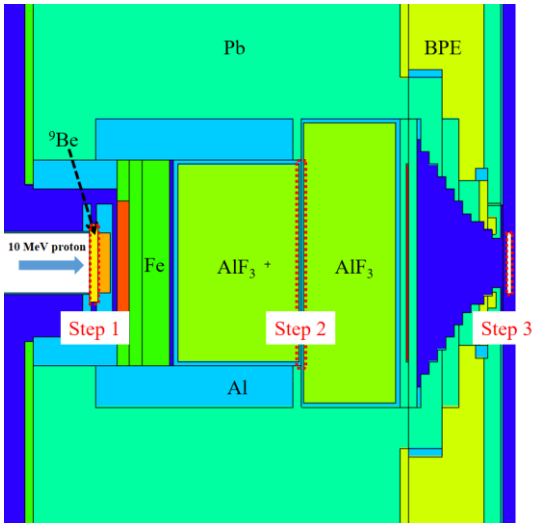

Fig. 1. The BSA design by PAL. The positions of each steps are red dotted.

2.2 BSA simulation

The Monte Carlo simulations for the BSA were done using MCNP6, PHITS and Geant4. The entire geometry of BSA was imported to simulation geometry with care.

The incident proton beam to the beryllium target was assumed as uniform field (12×12 cm^2) and mono energy (10 MeV). The three steps were applied splitting the simulation process and geometry into the three steps

making three phase-space files to reduce computing time. The first phase-space file collected all radiation passed through the beryllium target-end plane. Second phase-space file were recorded all radiation between the aluminum fluoride blocks. In the final step at the beam exit port, the neutron and photon which passed through the whole BSA materials were collected to make a phase-space file recording the position, direction, energy and particle name of each radiation. The three phase-space files were analyzed into the energy spectrum, radial flux and directionality.

2.3 Simple ^{9}Be target simulation and analytic calculation

The beryllium target geometry was taken out from the BSA without the other materials to compare the neutron yield. The simple target simulations were done using Geant4, PHITS and MCNP6. The proton beam were irradiated 12 × 12 cm^2 uniformly to the target and all of the protons are stopped in the target. The produced neutron and photon were recorded with their energy at the beryllium target surface. The target geometry is same as in the BSA and the condition of incident proton beam was also same with BSA simulation except for varying incident energy. The neutrons produced by ^{9}Be(p, n)^{9}B reaction were collected and their yield was analyzed by Monte Carlo and analytic calculation (Equation 1) [7].

$$\mathrm{Y}(E_b) = \int_{E_{thr}}^{E_b} \frac{\sigma(E)dE}{dE\ /\ dx} \quad (1)$$

Where E_b is the energy of incident proton beam, E_{thr} is threshold energy of the reaction, $\sigma(E)$ is the cross-section of ^{9}Be(p, n)^{9}B reaction, $dE\ /\ dx$ is the stopping power of proton beam.

For the analytic calculation, the cross-section data of ^{9}Be(p, n)^{9}B reaction were used from ENDF/B-VIII library [8] and stopping power data from NIST database by PSTAR [9]. Based on energy bin of NIST data, cross-section data were linearly interpolated.

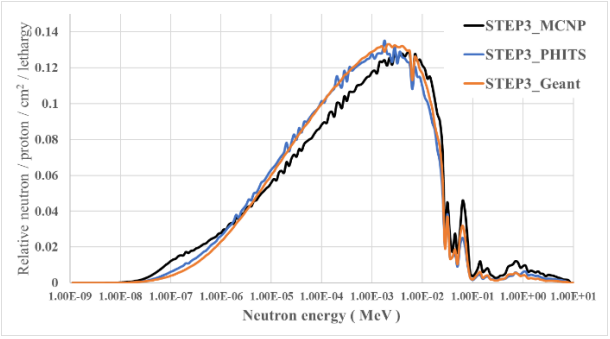

Fig. 2. The neutron energy spectrum at beam exit port by three different Monte Carlo codes. Graphs are normalized to have their Area Under Curve (AUC) is same, which means same number of neutrons are produced.

3. Results and discussion

3.1 Neutron beam characteristics

Figure 2 shows the neutron beam spectrum at the beam exit with three MC codes. The neutron beams are moderated passing through the BSA. In the fast and thermal neutron energy range, MCNP produced and transported more neutrons than other codes. However, in the epithermal range, MCNP showed smaller numbers of neutrons than other codes. Over 85% of neutrons are in the epithermal range at the beam exit. Figure 3and 4 shows the radial flux and directionality at the aperture whose final radius is 6 cm. The flux also steeply decreased after 6 cm apart.

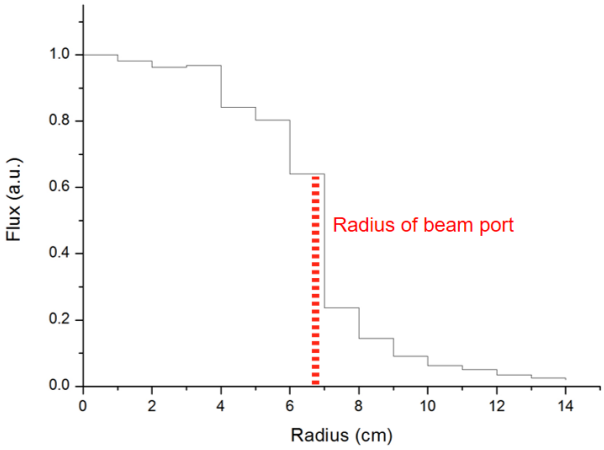

Fig. 3. The radial flux of neutron beam. The radius of beam exit port is 6 cm.

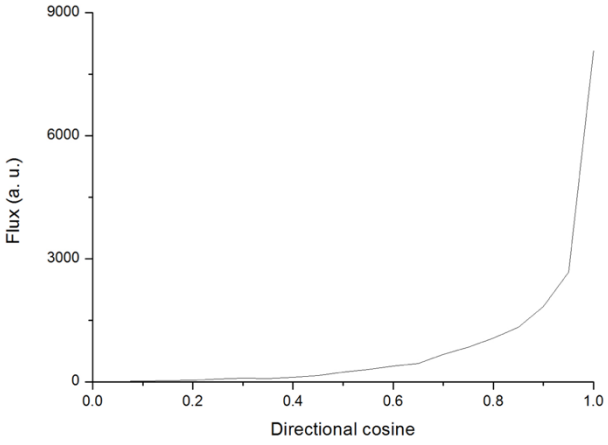

Fig. 4. The directional cosine of neutron beam. The directional cosine value which close to the one means that the beam is forwarded.

The neutron population during the three steps is shown in Figure 5. The step 1, which the neutron production process by ^{9}Be(p, n)^{9}B reaction is dominant showed the largest discrepancy. The MCNP showed around 7 times higher yield in the step 1. However, the neutron population decreased from step 1 to step 3 having similar trends with MC codes.

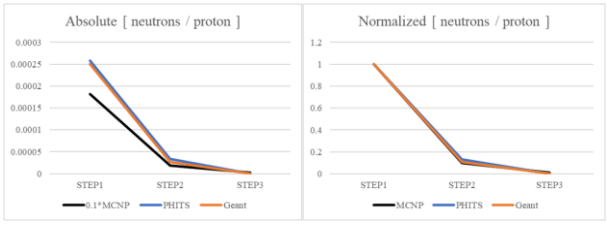

Fig. 5. The produced neutron per incident proton at step 1, 2 and 3. (left) Absolute neutron numbers per incident proton, MCNP results multiplied by 0.1 for comparison. (right) Normalized neutron numbers per incident proton, the values are normalized to step 1 for each codes.

3.2 Neutron yield

Figure 6 shows the energy spectrum of neutrons that emit from target surface. The neutrons produced in the MCNP showed higher average energy than other codes.

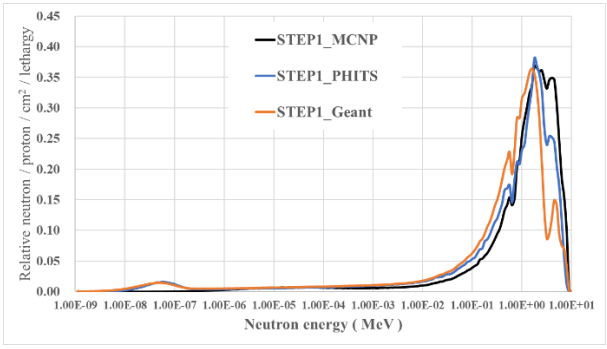

Fig. 6. The neutron energy spectrum by simple thick target with three different Monte Carlo codes. Graphs are normalized to have their Area Under Curve (AUC) is same, which means same number of neutrons are produced.

Figure 7 shows the neutron yield by Monte Carlo simulation, analytic calculation and experimental results from previous literature [10, 11]. The neutron yield by MCNP showed the most similar with analytic calculation and experiment but decreasing incident energy discrepancy increased. The other codes showed huge differences. These differences could the results that each MC codes uses different library for the cross-section data and different method to produce and transport in the codes. The MCNP used ENDF/B-VII.1 library for the cross-section data. In the Geant4, the physics list name "QGSP_BIC_HP" was used which uses evaluated nuclear data sets from TENDL-2014 and ENDF/B-VII.1 for the precise simulations of neutron and proton. The PHITS code uses JENDL library for the radiation transport.

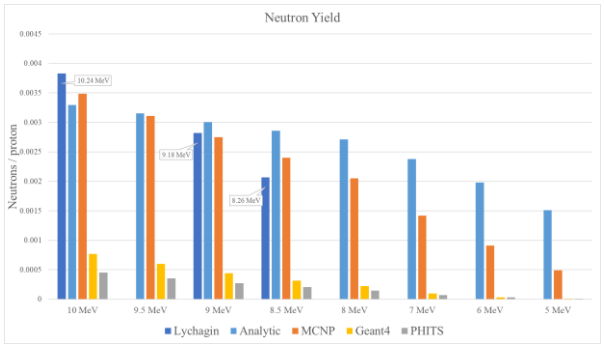

Fig. 7. The neutron yield comparison with Monte Carlo codes, analytic calculation and experimental data. The experimental data were at 10.24, 9.18 and 8.26 MeV of incident proton energy.

4. Conclusions

Although there are remaining issues in the beam assembly design to reduce fast neutrons, these neutron yield data and neutron spectra obtained by various MC codes could be used for the patient therapeutic dose calculation and initial input for the treatment planning system. The epithermal neutron flux for the current BSA met the IAEA guideline (i.e., 1×10^9 neutrons per sec-cm^2 in epithermal energy range, 2×10^{-13} Gy-cm2 per epithermal neutron for each fast neutron dose and gamma ray dose) [3]. The neutron yield by MCNP was the closest to both the analytic and experimental value. Therefore, the other codes need correction to their underestimated neutron yield to use in A-BNCT Monte Carlo simulations. In the near future, the comparison with measured data in the A-BNCT facility, such as neutron energy spectrum, thermal and fast neutron dose measurement, photon contamination, etc. will be done using paired ionization chambers and TLDs.

5. Acknowledgements

The authors thank to Sunggyun Shin, Ph.D. (PAL) for providing and revising design details of the BSA for this study.

REFERENCES

[1] W. A. Sauerwein, A. Wittig, R. Moss, Y. Nakagawa, Neutron Capture Therapy, Springer, Berlin, 2012
[2] R. Moss, Critical review with and optimistic outlook on Boron Neutron Capture Therapy (BNCT), Applied Radiation and Isotopes, Vol. 88, pp. 2-11, 2014.
[3] INTERNATIONAL ATOMIC ENERGY AGENCY, Current Status of Neutron Capture Therapy, IAEA-TECDOC-1223, IAEA, Vienna, 2001
[4] T. Goorley, *et al.*, Initial MCNP6 Release Overview, Nuclear Technology, 180, pp 298-315, 2012
[5] T. Sato, *et al.*, Features of Particle and Heavy Ion Transport code System (PHITS) version 3.02, J. Nucl. Sci. Technol., 2018
[6] Geant4—a simulation toolkit, Nuclear Instruments and Methods in Physics Research A, Vol. 506, pp. 250-303, 2003
[7] Eric B. Norman, et. al., Phys. Rev. C 30, 1339, 1984

[8] D.A.Brown, et al., ENDF/B-VIII.0: The 8th major release of the nuclear reaction data library with CIELO-project cross sections, new standards and thermal scattering data, Nucl. Data Sheets, Vol. 148, 2018
[9] M.J. Berger, J.S. Coursey, M.A. Zucker and J. Chang, Stopping-Power & Range Tables for Electrons, Protons, and Helium Ions, NIST Standard Reference Database 124, 2017
[10] A. A. Lychagin, B. V. Zhuravlev, V. G. Demenkov, U.A.Tchalyi, Conf: Int.Sem.on Interactions of Neutrons with Nuclei, No.10, p.333, 2003
[11] N. Otuka, et al., Towards a More Complete and Accurate Experimental Nuclear Reaction Data Library (EXFOR): International Collaboration Between Nuclear Reaction Data Centres (NRDC), Nucl. Data Sheets, Vol. 120, 2014